Bioinspired C/TiO$_2$ photocatalyst for rhodamine B degradation under visible light irradiation

Jian LI (✉)[1,2], Likun GAO[1,2], Wentao GAN[1,2]

1 Key Laboratory of Biobased Material Science & Technology of the Education Ministry,
Northeast Forestry University, Harbin 150040, China
2 Research Center of Wood Bionic Intelligent Science, Northeast Forestry University, Harbin 150040, China

Abstract *Papilio paris* butterfly wings were replicated by a sol-gel method and a calcination process, which could take advantage of the spatial features of the wing to enhance their photocatalytic properties. Hierarchical structures of *P. paris*-carbon-TiO$_2$ (PP-C-TiO$_2$) were confirmed by SEM observations. By applying the Brunauer-Emmett-Teller method, it was concluded that in the presence of wings the product shows higher surface area with respect to the pure TiO$_2$ made in the absence of the wings. The higher specific surface area is also beneficial for the improvement of photocatalytic property. Furthermore, the conduction and valence bands of the PP-C-TiO$_2$ are more negative than the corresponding bands of pure TiO$_2$, allowing the electrons to migrate from the valence band to the conduction band upon absorbing visible light. That is, the presence of C originating from wings in the PP-C-TiO$_2$ could extend the photoresponsiveness to visible light. This strategy provides a simple method to fabricate a high-performance photocatalyst, which enables the simultaneous control of the morphology and carbon element doping.

Keywords bioinspired, butterfly wings, C/TiO$_2$, photocatalyst, visible light

1 Introduction

The most commonly used photocatalysts such as TiO$_2$ with a band gap of 3.2 eV show relatively high reactivity and chemical stability under UV light. However, this part of the UV light spectrum ($\lambda < 387$ nm) accounts for only 4% of the solar energy[1]. This greatly limits the application of TiO$_2$ photocatalyst in practice. To use solar irradiation or interior lighting efficiently, many efforts have been made to seek a photocatalyst with high reactivity under visible light. One approach has been to dope nonmetal elements (e.g., C, N and P) into TiO$_2$, which could improve the optical response of TiO$_2$ under visible light excitation[2–5]. Irie et al. have reported a carbon-doped anatase TiO$_2$ powders generated by oxidizing commercial TiC powders, and the products showed photocatalytic activities for IPA decomposition under visible light (400–530 nm) irradiation[6]. This occurred because carbon occupied the oxygen sites and the substitution caused the absorbance edge of TiO$_2$ to shift to the higher wavelength region.

Moreover, researchers have found that the hierarchical structure is a significant feature contributing to high photocatalytic performance[7,8] because it can provide more active sites and enhance the capture efficiency of incident light[9]. In fact, natural materials possess an astonishing variety of hierarchical structures, which are not easily synthesized artificially. Song et al. fabricated an artificial N-doped ZnO photocatalyst by copying the elaborate architecture of green leaves through a two-steps infiltration and the N contained in the leaves self-doped into the products[10]. The artificial N-doped ZnO showed superior photocatalytic activity in the visible light region and excellent methylene blue degradation under solar energy irradiation. In addition to green leaves, there are many biotemplate materials in nature, such as bamboo, butterfly wings, cotton fibers, kelp, seaweed and wood[11–14]. Among these natural biotemplates, butterfly wings with uniform architecture often display special properties, such as high absorption range to visible light[13]. Furthermore, there are abundant biogenic C elements preserved in the wings.

Thus, we designed a simple method by using *Papilio paris* butterfly wings as biotemplates, coating with TiO$_2$ films and calcination in air to fabricate a *P. paris*-carbon-TiO$_2$ (PP-C-TiO$_2$) photocatalyst. In addition, the rhodamine B (RhB) photodegradation of the product was compared with that obtained with a measured amount of pure TiO$_2$.

2   Materials and methods

2.1   Materials

A *P. paris* butterfly sample was borrowed from Shanghai Natural Wild Insect Kingdom Co., Ltd. (Shanghai, China). *P. paris* butterfly wings were pretreated and washed with anhydrous ethanol, and dried in air for 12 h. All chemicals supplied by Shanghai Boyle Chemical Company (Shanghai, China) were of analytical reagent-grade quality and used without further purification. Deionized water was used throughout the study.

2.2   Synthesis

Moderate diethanol amine was added to a solution of a mixture of butyl titanate and anhydrous ethanol (molar ratio 17:1) with magnetic stirring. Subsequently, adequate 85% (w/w) ethanol aqueous solution was added dropwise to the solution with continuous stirring. The solution was magnetically stirred for > 3 h until the Tyndall phenomenon could be seen and a TiO_2 sol was obtained. The wings were carefully immersed into the TiO_2 sol for 20 h. The treated wings were then washed with deionized water and dried overnight at room temperature. The synthesis process is described in Fig. 1. The treated wings were calcined in air at 550°C for 3 h with a constant heating rate of $1°C \cdot min^{-1}$ to crystallize the TiO_2 and control the carbon content from the organic templates. The carbon content in the sample was about 0.6%. For comparison, pure TiO_2 was prepared through the same sol-gel method and calcination process without the wings.

2.3   Characterizations

The morphologies of the samples were characterized by field-emission scanning electron microscopy (FE-SEM, JSM-7500F, JEOL, Tokyo, Japan) operating at 12.5 kV in combination with energy dispersive spectroscopy (X-Max, Oxford Instruments, Abingdon, Oxfordshire, UK). The crystal structure of the as-prepared product was investigated by X-ray diffraction (D8 Advance, Bruker, Billerica, MA, USA) with Cu Kα radiation of wavelength λ = 1.5418 Å, using a step scan mode with the step size of 0.02° and a scan rate of $4° \cdot min^{-1}$, at 40 kV and 40 mA ranging from 5°

to 80°. Further evidence for the composition of the product was inferred from the specific surface area of the prepared products measured by the Brunauer-Emmett-Teller (BET) method based on N_2 adsorption at the temperature of liquid nitrogen using a 3H-2000PS2 unit (Beishide Instrument ST Co., Ltd, Beijing, China). Optical properties were characterized by the UV-vis diffuse reflectance spectroscopy (TU-190, Beijing Purkinje General Instrument Co., Ltd., Beijing, China) equipped with an integrating sphere attachment, using $BaSO_4$ as the reference. Thermogravimetric analysis was carried on using a simultaneous thermal analyzer (SDT Q600, TA Instruments, New Castle, DE, USA) in a temperature range of 25–700°C under a dynamic N_2 atmosphere.

2.4   Photocatalytic test

For photocatalytic tests, a measured quantity of sample was dissolved in 100 mL aqueous solutions of RhB in glass beakers. The concentration of RhB was 10 mg in 1 L of H_2O. At first, the solution was stirred continuously in the dark for 60 min to establish adsorption-desorption equilibrium among the photocatalysts and dye solution, then this solution was illuminated with visible light. A 500 W xenon lamp with the wavelength range of 425 nm was used as light source and the intensity of the incident visible light on the solution was 110 $W \cdot m^{-2}$. The glass beaker was then placed in front of the lamp with continuous magnetic stirring. Five ml of solution was collected and centrifuged. The UV absorption measurements were then used to observe the photodegradation at specific time intervals. The absorption peaks for RhB were observed at 553 nm. Stability of the material was measured in the solution with the above steps repeated four times.

3   Results and discussion

SEM images of the original butterfly wings, TiO_2-treated wings and PP-C-TiO_2 are presented in Fig. 2. The wings had a well-organized porous framework and a hierarchical architecture assembled in ridges and pillars (Fig. 2a). After treatment with TiO_2 sol, the pores were all filled (Fig. 2b). Through the calcination in air, the PP-C-TiO_2 faithfully replicated the well-organized porous hierarchical architecture of the natural wings (Fig. 2c).
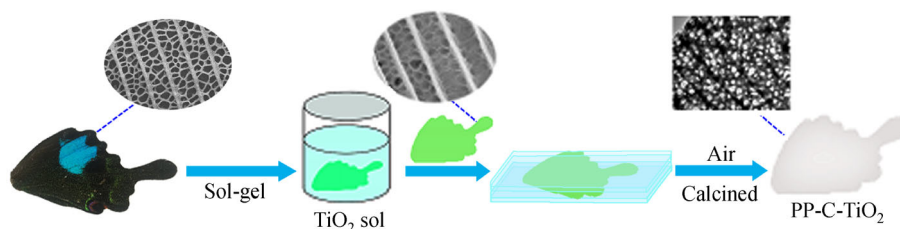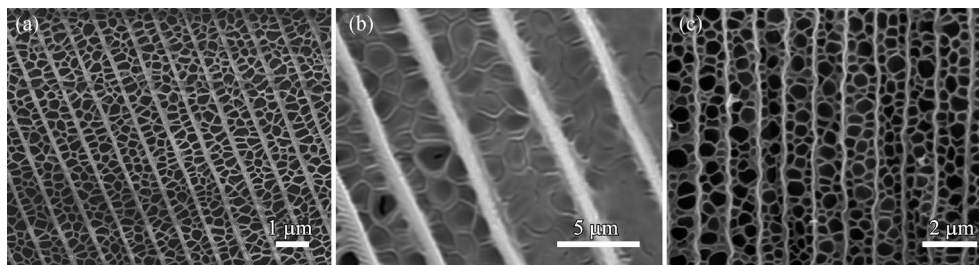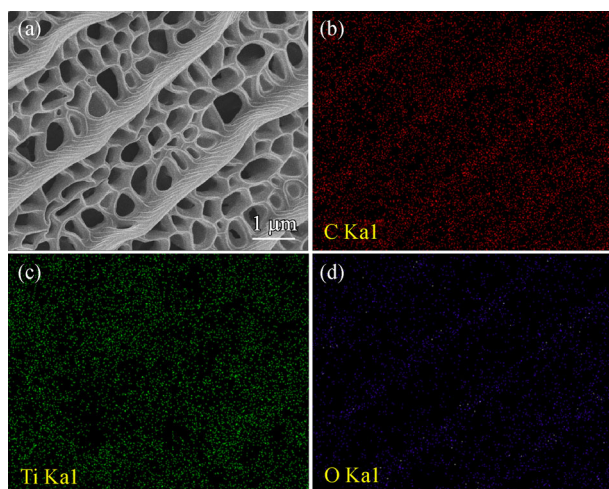

Fig. 1   Synthesis of TiO_2-replicated *Papilio paris* wings (PP-C-TiO_2)

Fig. 2 SEM images of original *Papilio paris* butterfly wings (a), TiO$_2$-treated *P. paris* wings (b), and TiO$_2$-replicated wings (PP-C-TiO$_2$) (c)
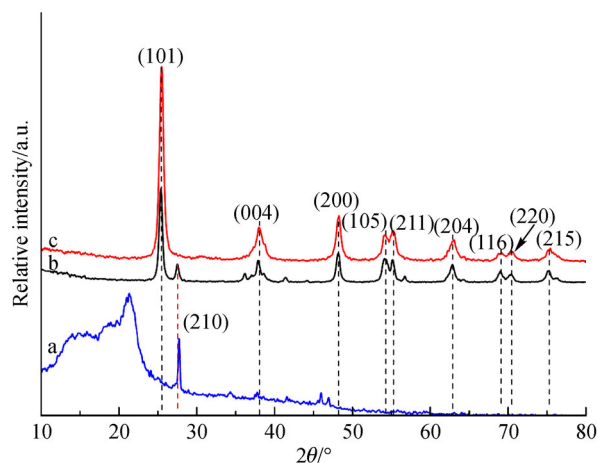
The distributions of C, O and Ti in the PP-C-TiO$_2$ are presented by element mapping in Fig. 3. The C present came from the wing exoskeleton, whereas the O and the Ti were mainly from the added TiO$_2$. Element mapping also indicated that Ti and O were uniformly distributed after calcination in air.
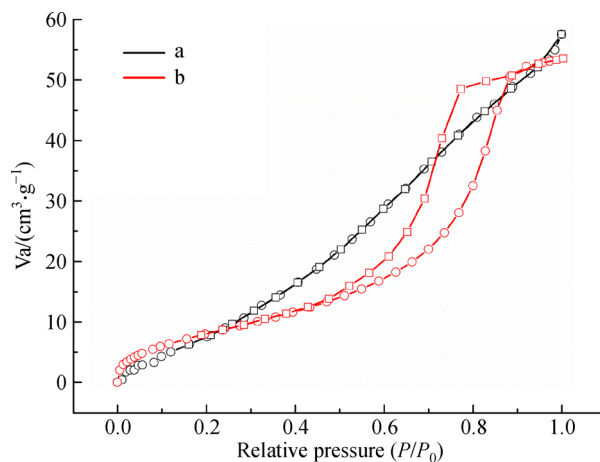

Fig. 3 SEM images (a) and C (b), Ti (c) and O (d) element mappings of the TiO$_2$-replicated *Papilio paris* wings (PP-C-TiO$_2$)

Fig. 4 X-ray diffraction patterns of TiO$_2$-treated butterfly wings (a), pure TiO$_2$ (b), and TiO$_2$-replicated *Papilio paris* wings (PP-C-TiO$_2$) (c)

Figure 4 shows the X-ray diffraction patterns of the TiO$_2$-treated wings, the pure TiO$_2$ and the PP-C-TiO$_2$. The diffraction peaks at 28.4° (Fig. 4a, Fig. 4b) belong to the (210) crystal planes of TiO$_2$. The diffraction peaks of the pure TiO$_2$ are well indexed to the standard diffraction pattern of anatase phase TiO$_2$ (JCPDS file no. 21-1272)[15,16]. After calcination in air, the diffraction peaks of the PP-C-TiO$_2$ (Fig. 4c) were the same as the pure TiO$_2$ (Fig. 4b). The curves in Fig. 4b and Fig. 4c show the peaks center at 2θ = 25.2°, 38.0°, 47.8°, 54.2°, 55.3°, 62.5°, 68.8°, 70.5° and 74.9°, which agrees with the (101), (004), (200), (105), (211), (204), (116), (220) and (215) crystal planes of anatase TiO$_2$.

BET analysis was conducted in order to understand the effect of the wings on the porous structure of the samples. Figure 5 shows the N$_2$ adsorption-desorption isotherms of the pure TiO$_2$ and the PP-C-TiO$_2$. It could be seen the

Fig. 5 N$_2$ adsorption-desorption isotherms of pure TiO$_2$ (a) and TiO$_2$-replicated *Papilio paris* wings (PP-C-TiO$_2$) (b)

curve for the PP-C- TiO$_2$ exhibits a hysteresis loop, which is attributed to type IV isotherms and the representative of mesoporous materials, indicating the presence of meso-pores (2–50 nm)[17,18], while the curve for the pure TiO$_2$

shows a type III isotherm, which indicates that the absorption property of the material is weak.

BET surface areas, pore sizes and pore volumes of the pure TiO_2 and the PP-C-TiO_2 are presented in Table 1. From these data, it is clear that the preparation of TiO_2 in the presence of the wings after calcination produced a significantly higher (up to 1.7 times) surface area than the pure TiO_2. The pure TiO_2 had a relatively low surface area of 29.7 $m^2 \cdot g^{-1}$. The sample prepared in the presence of the wings, S_{BET} is higher than 50 $m^2 \cdot g^{-1}$. That is, the method used seems to have produced a certain heterogeneous system with respect to the wings, in terms of the surface properties (e.g., surface area and pore size distribution) of the PP-C-TiO_2. Thus, because of its large surface area, the PP-C-TiO_2 provides more photocatalytic reaction sites for the adsorption of reactant molecules and increases the efficiency of the electron-hole separation, so the photocatalytic activity of the PP-C-TiO_2 is enhanced.

Table 1 Structural parameters of pure TiO_2 and TiO_2-replicated *Papilio paris* wings (PP-C-TiO_2)

Sample	BET surface area /($m^2 \cdot g^{-1}$)	Pore size /nm	Pores volume /($cm^3 \cdot g^{-1}$)
Pure TiO_2	29.7	11.20	0.08
PP-C-TiO_2	51.9	9.05	0.12

To investigate the light absorbance of the samples, the UV-vis diffuse reflection spectra of the pure TiO_2 and the PP-C-TiO_2 were obtained (Fig. 6a). For the pure TiO_2, there was prominent adsorption below 350 nm, whereas for the PP-C-TiO_2 there was a much higher absorption in the region 380–500 nm, indicating the absorption of PP-C-TiO_2 is significantly red-shifted to visible wavelengths, due to the presence of C. Moreover, it is worth noting that the PP-C-TiO_2 heterostructures with absorptions in the visible region may indicate a greater potential for photocatalysis. To calculate valence band position, the

optical band gap was determined by the following Tauc equation[19]:

$$(\alpha h\nu)^n = A(h\nu - E_g)$$

where A = constant, $h\nu$ = light energy, E_g = optical band gap energy, α = measure absorption coefficient, and $n = 0.5$ for indirect band gap. Given that TiO_2 has an indirect band gap, the y axis of the Tauc plot is $(\alpha h\nu)^{1/2}$ for TiO_2[20]. In Fig. 6b, the extrapolation of the Tauc plot to x intercepts gives optical band gaps of 3.02 eV and 2.23 eV for the pure TiO_2 and the PP-C-TiO_2, respectively. Therefore, the conduction band and valence band of the PP-C-TiO_2 are more negative than the corresponding bands of the pure TiO_2. It is possible for the electrons to migrate from the valence band to the conduction band upon absorbing visible light, which could lead to the visible light activity of the PP-C-TiO_2.

To test the photodegradation abilities of the samples, the photocatalytic degradation of RhB was measured. Figure 7a shows the relationships between concentration ratio (C/C_0) and time for RhB degradation with 50 mg pure TiO_2, 50 mg PP-C-TiO_2 and irradiation without photocatalysts. The PP-C-TiO_2 took 90 min to degrade phenol. However, the pure TiO_2 could not degrade RhB. Figure 7b shows the first order rate constant k (min^{-1}) of the pure TiO_2 and the PP-C-TiO_2 for RhB, which was calculated by the following first order equation[21,22]:

$$\ln(C_0/C) = kt$$

where C_0 is the initial concentration of the dye in solution and C is the concentration of dye at time t. This shows the k value of 0.02614 min^{-1} for RhB in the case of the pure TiO_2 as compared to the value of 0.00039 min^{-1} in the case of the PP-C-TiO_2. This indicates that the PP-C-TiO_2 possesses photodegradation abilities.

PP-C-TiO_2 as a photocatalyst can easily be recycled by a simple filtration. After four cycles for the photodegradation of RhB, the catalyst did not exhibit any significant loss of
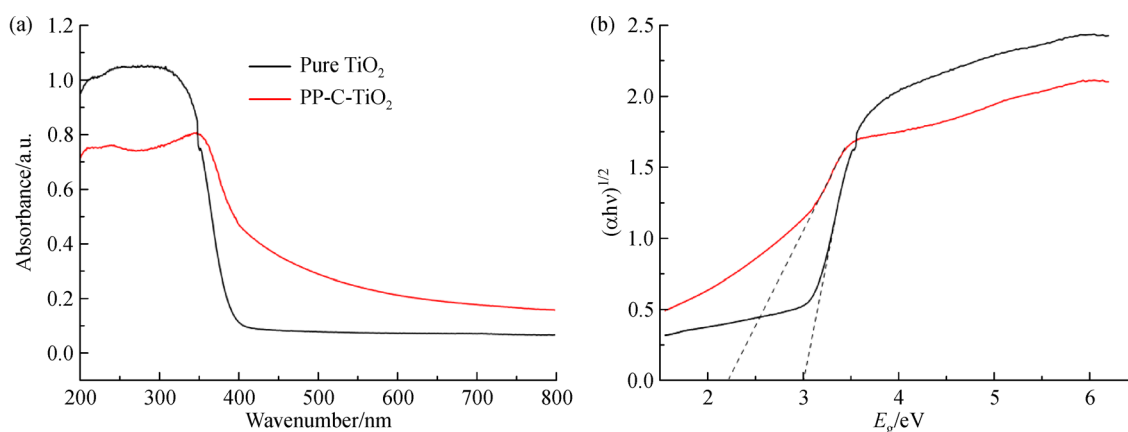

Fig. 6 (a) UV-vis absorption spectra of the pure TiO_2 and TiO_2-replicated *Papilio paris* wings (PP-C-TiO_2); (b) the evaluation of the optical band gap using the Tauc plot.
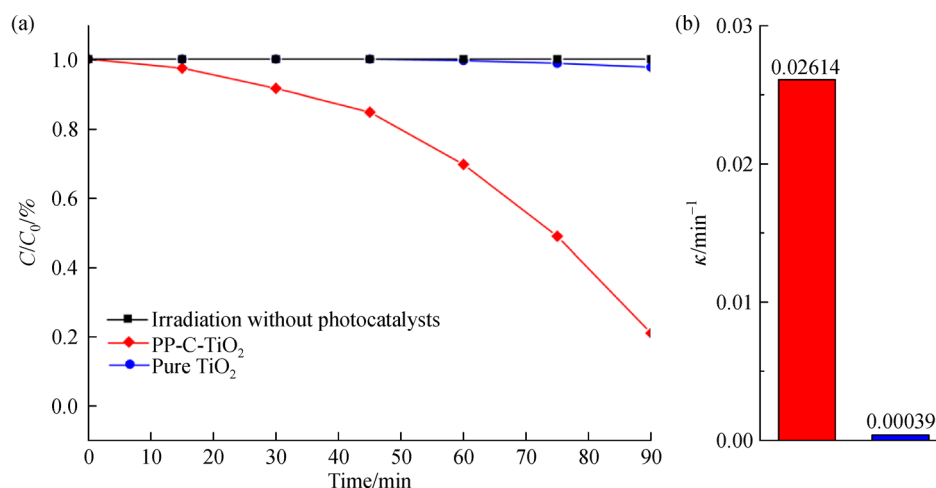
Fig. 7   (a) Concentration ratio (C/C_0) of photocatalytic rhodamine B with pure TiO$_2$, TiO$_2$-replicated *Papilio paris* wings (PP-C-TiO$_2$) and irradiation without photocatalysts; (b) first order rate constant k (min^{-1}) of pure TiO$_2$ and PP-C-TiO$_2$ for RhB.

activity (Fig. 8), confirming that the PP-C-TiO$_2$ is not photocorroded during the photocatalytic oxidation of the dye pollutant. Therefore, this stable photocatalyst show a great potential for practical applications.
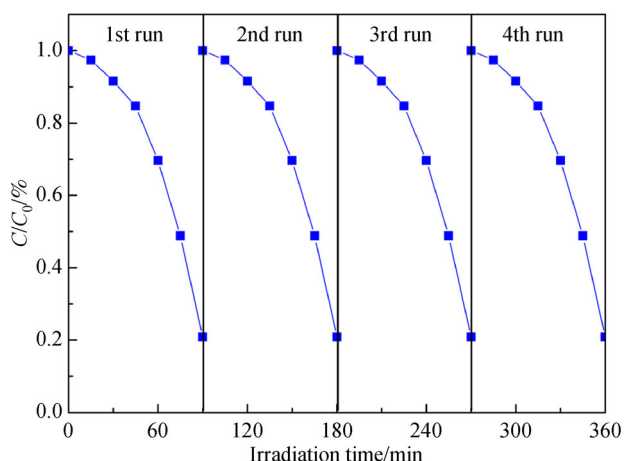
Fig. 8   Comparison of repeated cycles of photocatalytic degradation of rhodamine B in the presence of 50 mg TiO$_2$-replicated *Papilio paris* wings (PP-C-TiO$_2$) under visible irradiation

4   Conclusions

A sol-gel method and a calcination process were combined to fabricate heterostructured C/TiO$_2$ photocatalysts from *P. paris* butterfly wings. The elaborate architecture of the wings was copied by immersing the wings into the TiO$_2$ sol, followed by calcination in air to remove the wings. Moreover, the C contained in the wings was self-doped into the products. These *P. paris*-C-TiO$_2$ exhibited high potential for application as a visible light photocatalyst for degradation of organic pollutants. This is ascribed to the hierarchical structures and the higher surface area that

provide more reactive sites for photocatalysis. Also, the C dopant decreases the band gap of TiO$_2$ and shifts the optical absorption to the visible light region. This work provides a pathway for constructing high-performance materials and efficiently utilizing of solar energy.

Compliance with ethics guidelines   Jian Li, Likun Gao, and Wentao Gan declare that they have no conflicts of interest or financial conflicts to disclose.

This article does not contain any studies with human or animal subjects performed by any of the authors.

References

1. Vernardou D, Drosos H, Spanakis E, Koudoumas E, Savvakis C, Katsarakis N. Electrochemical and photocatalytic properties of WO$_3$ coatings grown at low temperatures. *Journal of Materials Chemistry*, 2011, **21**(2): 513–517

2. Asahi R, Morikawa T, Ohwaki T, Aoki K, Taga Y. Visible-light photocatalysis in nitrogen-doped titanium oxides. *Science*, 2001, **293**(5528): 269–271

3. Khan S U M, Al-Shahry M, Ingler W B Jr. Efficient photochemical water splitting by a chemically modified n-TiO$_2$. *Science*, 2002, **297** (5590): 2243–2245

4. Lin L, Zheng R Y, Xie J L, Zhu Y X, Xie Y C. Synthesis and characterization of phosphor and nitrogen co-doped titania. *Applied Catalysis B: Environmental*, 2007, **76**(1–2): 196–202

5. Ohno T, Tsubota T, Nishijima K, Miyamoto Z. Degradation of methylene blue on carbonate species-doped TiO$_2$ photocatalysts under visible light. *Chemistry Letters*, 2004, **33**(6): 750–751

6. Irie H, Watanabe Y, Hashimoto K. Carbon-doped anatase TiO$_2$ powders as a visible-light sensitive photocatalyst. *Chemistry Letters*, 2003, **32**(8): 772–773

7. Parlett C M A, Wilson K, Lee A F. Hierarchical porous materials: catalytic applications. *Chemical Society Reviews*, 2013, **42**(9): 3876–3893

8. Cho K, Na K, Kim J, Terasaki O, Ryoo R. Zeolite synthesis using hierarchical structure-directing surfactants: retaining porous structure of initial synthesis gel and precursors. *Chemistry of Materials*, 2012, **24**(14): 2733–2738

9. Yin C, Zhu S, Chen Z, Zhang W, Gu J, Zhang D. One step fabrication of C-doped $BiVO_4$ with hierarchical structures for a high-performance photocatalyst under visible light irradiation. *Journal of Materials Chemistry A: Materials for Energy and Sustainability*, 2013, **1**(29): 8367–8378

10. Song F, Su H, Han J, Zhang D, Chen Z. Fabrication and good ethanol sensing of biomorphic SnO_2 with architecture hierarchy of butterfly wings. *Nanotechnology*, 2009, **20**(49): 495502

11. Shi N, Li X, Fan T, Zhou H, Ding J, Zhang D, Zhu H. Biogenic NI-codoped TiO_2 photocatalyst derived from kelp for efficient dye degradation. *Energy & Environmental Science*, 2011, **4**(1): 172–180

12. Song M Y, Park H Y, Yang D S, Bhattacharjya D, Yu J S. Seaweed-derived heteroatom-doped highly porous carbon as an electrocatalyst for the oxygen reduction reaction. *ChemSusChem*, 2014, **7**(6): 1755–1763

13. Li Y, Meng Q, Ma J, Zhu C, Cui J, Chen Z, Guo Z, Zhang T, Zhu S, Zhang D. Bioinspired carbon/SnO_2 composite anodes prepared from a photonic hierarchical structure for lithium batteries. *ACS Applied Materials & Interfaces*, 2015, **7**(21): 11146–11154

14. Peng W, Hu X, Zhang D. Bioinspired fabrication of magneto-optic hierarchical architecture by hydrothermal process from butterfly wing. *Journal of Magnetism and Magnetic Materials*, 2011, **323** (15): 2064–2069

15. Gao L, Gan W, Xiao S, Zhan X, Li J. Enhancement of photocatalytic degradation of formaldehyde through loading anatase TiO_2 and silver nanoparticle films on wood substrates. *RSC Advances*, 2015, **5**(65): 52985–52992

16. Gao L, Qiu Z, Gan W, Zhan X, Li J, Qiang T. Negative oxygen ions production by superamphiphobic and antibacterial TiO_2/Cu_2O composite film anchored on wooden substrates. *Scientific Reports*, 2016, **6**(1): 26055–26064

17. Gao L, Gan W, Qiu Z, Zhan X, Qiang T, Li J. Preparation of heterostructured WO_3/TiO_2 catalysts from wood fibers and its versatile photodegradation abilities. *Scientific Reports*, 2017, **7**(1): 1102–1114

18. Tahir M, Cao C, Butt F K, Butt S, Idrees F, Ali Z, Aslam I, Tanveer M, Mahmood A, Mahmood N. Large scale production of novel gC_3N_4 micro strings with high surface area and versatile photodegradation ability. *CrystEngComm*, 2014, **16**(9): 1825–1830

19. Mor G K, Varghese O K, Paulose M, Grimes C A. Transparent highly ordered TiO_2 nanotube arrays via anodization of titanium thin films. *Advanced Functional Materials*, 2005, **15**(8): 1291–1296

20. Satoh N, Nakashima T, Kamikura K, Yamamoto K. Quantum size effect in TiO_2 nanoparticles prepared by finely controlled metal assembly on dendrimer templates. *Nature Nanotechnology*, 2008, **3** (2): 106–111

21. Han C, Wang Y, Lei Y, Wang B, Wu N, Shi Q, Li Q. *In situ* synthesis of graphitic-C_3N_4 nanosheet hybridized N-doped TiO_2 nanofibers for efficient photocatalytic H_2 production and degradation. *Nano Research*, 2015, **8**(4): 1199–1209

22. Zhao S, Chen S, Yu H, Quan X. gC_3N_4/TiO_2 hybrid photocatalyst with wide absorption wavelength range and effective photogenerated charge separation. *Separation and Purification Technology*, 2012, **99**: 50–54